Statistical *n*-Butyl Acrylate–(Sulfopropyl)ammonium Betaine Copolymers. 2. Structural Studies

Marc Ehrmann, André Mathis, Bernard Meurer, Monique Scheer, and Jean-Claude Galin*

Institut Charles Sadron (CRM–EAHP), CNRS–ULP, 6 rue Boussingault, 67083 Strasbourg Cedex, France

Received June 3, 1991; Revised Manuscript Received November 14, 1991

ABSTRACT: The structural analysis of a series of amorphous statistical copolymers of *n*-butyl acrylate (A) and dimethyl(3-methacrylamidopropyl)(3-sulfopropyl)ammonium betaine (B) was performed through differential scanning calorimetry (DSC), small-angle X-ray scattering (SAXS), and solid-state NMR spectroscopy (^{1}H broad line and ^{13}C high resolution). In copolymers of low and moderate B content [0.04 < F_B (molar fraction) < 0.35] strong dipolar interactions between the zwitterionic units ($\mu \simeq 25$ D) result in a typical biphasic structure. DSC clearly shows two well-separated glass transitions, allowing a quantitative description of the copolymer morphology in terms of a soft matrix (−46 < T_g^S (°C) < −20) containing only very low amounts of B units (F_B^S < 0.07) and hard domains (30 < T_g^H (°C) < 120) containing rather high amounts of A units (0.45 < F_A^H < 0.73). Solid-state NMR analysis confirms the fair purity of the mobile phase and the chemical heterogeneity of the rigid phase, which may be quantitatively correlated with the hard domains identified in DSC. The presence of a single SAXS peak and the variations of the corresponding Bragg spacings d (4–7 nm) according to a power law of the type $d \propto \Phi_B^{-0.27}$ (Φ_B = volume fraction of B units) suggest a random distribution of the dipolar scattering entities within the apolar matrix. A low fraction of the zwitterions still remain strongly associated in rigid aggregates stable at very high temperatures such as T_g^H + 100 °C. With respect to phase separation, the zwitterionic copolymers may appear as a very versatile alternative to the corresponding quaternary ammonium cationic ionomers.

Introduction

In the first part of this series[1] we reported the synthesis and the molecular characterization of statistical amorphous copolymers of *n*-butyl acrylate (A) and dimethyl(3-methacrylamidopropyl)(3-sulfopropyl)ammonium betaine (B):

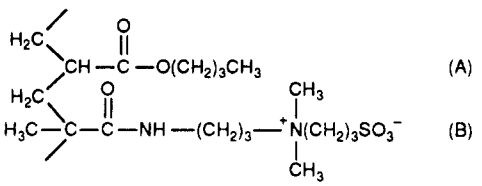

By analogy with the closely related ethyl acrylate–(sulfopropyl)ammonium betaine copolymers studied previously,[2-4] with literature results on other statistical,[5-10] telechelic,[11] or zwitterionic copolymers, and, finally, with well-known ionomers,[11-16] the bulk copolymers of low or moderate zwitterion content are expected to show a very specific biphasic structure characterized by a dispersion of B-rich microdomains within a B-poor matrix: obviously, the very likely strong dipolar interactions between the zwitterionic units[17] (μ = 25 D for $(C_2H_5)_3N^+(CH_2)_3SO_3^-$ [18]), and the fairly low polarity ($(\mu^2/N)^{0.5}$ = 1.85 D[19]) and the high mobility (T_G = −46 °C) of the *n*-butyl acrylate matrix, would favor microphase separation in such materials. The present work is devoted to the structural and morphological characterization of the zwitterionic copolymers in bulk by three complementary techniques: differential scanning calorimetry (DSC), wide- and small-angle X-ray scattering (WAXS and SAXS), and solid-state NMR spectroscopy (^{1}H broad line and ^{13}C high resolution). While DSC appears as a global method sensitive to structural heterogeneities on a rather large scale, SAXS tests the material homogeneity on a substantially lower scale, and the NMR techniques provide useful information on both chain dynamics and composition on a local level for polyphasic materials.

Compared to the large number of studies devoted to ionomers,[12-16] work on statistical zwitterionic copolymers has been quite modest. Still, these polymers with strongly interacting lateral groups randomly distributed along the backbone are of considerable interest both for basic studies and for potential technological applications.

Experimental Section

Synthesis of the Statistical Copolymers. The copolymers were obtained by radical-initiated copolymerization of *n*-butyl acrylate (A) and dimethyl(3-methacrylamidopropyl)(sulfopropyl)ammonium betaine (B) monomers (r_A = 0.42, r_B = 6.0 at 50 °C) restricted to low conversion (<20%) as described elsewhere.[1] The stoichiometric blends of copolymers with $LiClO_4$ ([$LiClO_4$]/[B] = 1) were obtained by evaporation of their dilute solutions in trifluoroethanol. All the samples used for the structural studies were dried to constant weight at 80 °C under 10^{-2} Torr (≃1.3 Pa) for 24 h before any experiment.

Differential Scanning Calorimetry (DSC). The glass transition temperatures, T_g, were measured with a Perkin-Elmer DSC-2 or a Perkin-Elmer DSC-4 apparatus interfaced with a computer data station, using either 10–20-mg samples in the usual aluminum pan or 25–35-mg samples in O-ring stainless steel large-volume capsules (water-tight joint). The following heating–cooling sequences were systematically repeated until reproducible scans were obtained (most often the third one for the low transition and the fourth one for the high transition): heating to T_g + 100 °C at a rate of 20 °C min^{-1}, annealing for 10 min at this temperature, cooling to a low temperature, depending on the polymer glass transition, at a rate of 40 °C min^{-1}, and annealing for 5 min. The transition temperature was determined as the midpoint of the baseline shift ($\Delta C_p/2$). The transition width was estimated by $\Delta T = T_2 - T_1$, where T_1 and T_2 are the intersections of the extrapolated glassy and liquid baselines with the tangent to the thermogram inflection point.

Wide- and Small-Angle X-ray Scattering (WAXS and SAXS). WAXS and SAXS experiments were carried out between −40 and +180 °C with the usual experimental device[20] operating with a linear collimation of a monochromatic X-ray beam of λ = 0.154 nm of large height and fitted with a linear detector for quantitative analysis. The previously dried samples were directly transferred to the sample holder for X-ray mea-

0024-9297/92/2225-2253$03.00/0

Table I
Glass Transitions and Composition Data of the Various Copolymers As Derived from DSC

copolymer	W_B	T_g, °C	ΔC_p, J·g^{-1}·K^{-1}	W^S	W_B^S	W_B^H
A	0	−46.5	0.335	1		
		—				
AB-2.0	0.045	−43.2	0.343	1		
		—				
AB-4.0	0.087	−40.1	0.280	1		
		—				
AB-4.6	0.098	−41.7	0.251	0.840	0.030	0.453
		+33	0.042			
AB-7.1	0.148	−37.7	0.226	0.798	0.060	0.498
		+44	0.067			
AB-7.1 + $LiClO_4$[a]	0.148	−37.1	0.238			
		+59	0.100			
AB-9.7	0.197	−35.1	0.209	0.685	0.081	0.449
		+32	0.075			
AB-10.9	0.218	−35.1	0.209	0.713	0.081	0.558
		+60	0.075			
AB-11.3	0.225	−36.0	0.184	0.683	0.074	0.551
		+58	0.067			
AB-12.0 fraction[b]	0.236	−33.9	0.184	0.695	0.088	0.573
		+64	0.105			
AB-12.0[c]	0.237	−32.7	0.167	0.700	0.095	0.569
		+63	0.096			
AB-12.8	0.250	−36.5	0.197	0.613	0.074	0.529
		+52	0.079			
AB-15.6	0.297	−31.3	0.155	0.651	0.109	0.648
		+87	0.096			
AB-27.3	0.462	−26.0	0.113	0.459	0.142	0.733
		+117	0.130			
AB-48.9	0.686	—	—	0		
		+156	0.146			
AB-88.6	0.946	—	—	0		
		+237[d]	0.171			

[a] $[LiClO_4]/[B] = 1$, amorphous blend. [b] Fractionated copolymer: $M_w = 4.9 \times 10^4$, $M_w/M_n = 1.24$. [c] Unfractionated copolymer: $M_w = 9.2 \times 10^4$, $M_w/M_n = 1.75$. [d] Estimated value just before thermal degradation.

surements. Molding of the sample at 100 °C under vacuum does not lead to any significant change in the SAXS patterns.

Specific volumes at 25 °C of the homopolymers A_n and B_n were 0.944 and 0.721 mL g^{-1}, respectively, as taken from literature[21] for A_n and from partial specific volume measurements in H_2O–0.1 N $LiClO_4$ solution for B_n (Anton Paar KG digital densitometer, Model DMA-02).

Solid-State NMR Techniques. ^{1}H Wide-Line Analysis. Solid-state NMR line shape analysis was performed on a Bruker SXP spectrometer operating at 60 MHz. Signals were digitized with 8 bits (accuracy of 1/100) at a fastest sampling rate of 10 MHz (Bruker BC 100 q) or with 12 bits (accuracy of 1/2000) at a fastest sampling rate of 5 MHz (Le Croy 6810). In each converter, memory is filled at a lower sampling rate to obtain simultaneously an accurate base line and the slowly decaying component (samplings between 100 kHz and 1 MHz). A signal/noise ratio of 500 by digital averaging was typical for adjusting sums of exponentials (≤2 components) by iterative least squares nonlinear fits. Polynomial[22] or Gaussian functions were adjusted to the fast decaying part of the fid, allowing extrapolation through the 7-μs dead time to the origin of the fid (taken at the middle of the 90° rf pulse).

^{13}C High Resolution. ^{1}H–^{13}C cross-polarization, proton dipolar decoupling, and magic angle spinning (CP/DD/MAS) NMR experiments were performed at 50.3 MHz on a Bruker CXP 200 fitted with a 7-mm, double-bearing, variable-temperature probe (Bruker). The matched spin-lock cross-polarization and decoupling involved ^{13}C and ^{1}H magnetic field strengths of 40 kHz. To avoid water moisture, the rotor was driven by N_2 gas from a liquid nitrogen evaporator (Cryodiffusion EMP 160).

The spectrum of the mobile (non cross-polarizable) phase was recorded by 90° ^{13}C excitation and ^{1}H broad-band decoupling using a repetition time of 3 s.

Results and Discussion

The copolymers (see Experimental Section) were chemically homogeneous,[1] had fairly high degrees of polymerization ($1000 < DP_w < 2300$), and had reasonable molecular weight distributions ($M_w/M_n \simeq 1.7$–2.2).

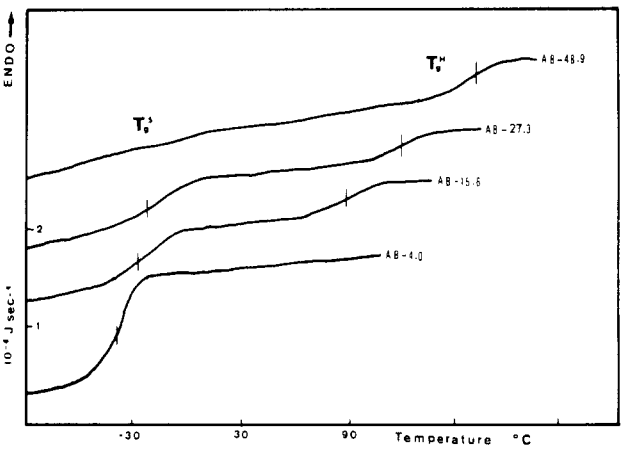

Figure 1. Representative DSC thermograms of various monophasic or biphasic copolymers.

In the following text, F_i, W_i, and Φ_i will refer to the molar fraction, the weight fraction, and the volume fraction of component i in the copolymers, which are denoted as AB followed by a figure related to their molar composition: For instance, AB-7.1 is a copolymer containing 7.1 mol % of B units.

Differential Scanning Calorimetry Measurements. The DSC results are shown in Table I. Three types of behavior may be recognized depending on the zwitterion content of the copolymer (Figure 1).

(a) For $W_B < 0.10$ ($F_B < 0.046$), a single transition is observed: the corresponding "low-temperature" T_g is well reproducible and defined with a good accuracy (±1.5 °C), and the transition is fairly sharp ($\Delta T \simeq 12 \pm 2$ °C).

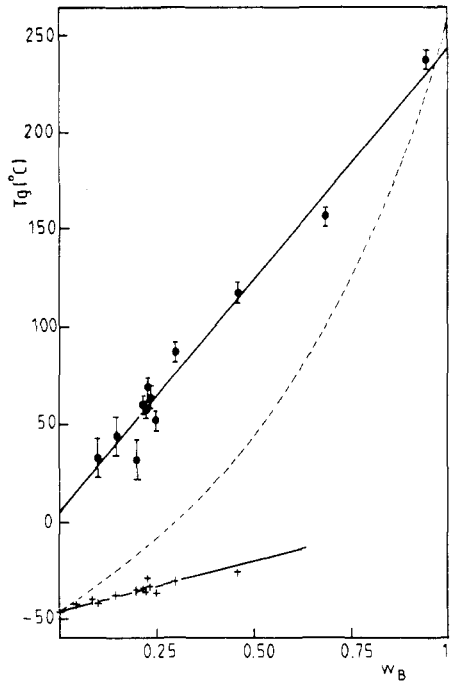

Figure 2. Composition dependence of the glass transition temperatures of the AB copolymers.

(b) For $0.10 \leq W_B \leq 0.65$ ($0.046 \leq F_B < 0.449$), two well-separated transitions are observed, as shown in Figure 1 for two representative copolymers. In this composition range, the transition width ΔT ($\Delta T \simeq 16$–28 °C) for the "low" T_g is significantly increased with respect to the previous case, and that of the "high" T_g is still broader ($\Delta T \simeq 20$–45 °C): this feature suggests an enhanced compositional distribution of the chain segments involved in this latter transition (see further). Moreover, quenching the sample from the liquid state ("high" T_g + 100 °C) down to −130 °C at the fastest cooling rate of 320 K min^{-1} before running the thermogram does not yield any significant change in both transitions compared to the usual cooling rate of 40 K min^{-1}. For various samples of the same copolymer dried under the same conditions and for identical DSC cycles (see Experimental Section), the reproducibility of the "low" T_g remains fairly good (±1.5 °C) while that of the "high" T_g is definitely worse and composition dependent: ±5 °C for the copolymers with the higher B content ($W_B > 0.2$), and only ±10 °C for the copolymers with the lower B content ($W_B < 0.2$). We have no satisfactory explanation for this behavior. Finally, molecular weight and molecular weight distribution have no significant effect on either transition: compare for instance the two runs AB-12.0 in Table I.

(c) For $W_B > 0.65$ ($F_B > 0.449$), only a single "high-temperature" T_g is observed.

The most striking feature of all these DSC results plotted in Figure 2 is the occurrence of two clearly separated glass transitions for the copolymers of intermediate zwitterion content. This is indeed very unusual for such materials: only a single T_g has been observed over the whole composition range for the closely related ethyl acrylate–zwitterionic system[3] or for some other zwitterionic copolymers described in the literature.[7,10] To the best of our knowledge, only styrene–sodium styrenesulfonate (0.18 mole fraction of the salt unit) shows two well-separated T_g's in DSC experiments.[23] Moreover, for our system, no noticeable event can be detected in the DSC traces at temperatures above the "high" T_g up to the thermal degradation of the samples (≃250 °C), in sharp contrast with the endotherm reported recently for a series of zwitterionic copolymers of alkyl methacrylates.[10] Both T_g's increase with the zwitterion content (see Figure 2), but much more rapidly for the higher one, and their variations may be correlated (regression coefficient R) with copolymer composition according to the following:

$$\text{for } 0 < W_B < 0.46, \text{ "low" } T_g\text{:}$$

$$T_g\ (°C) = -46.4 + 52.3W_B;\quad R(13) = 0.981$$

$$\text{for } 0.098 < W_B < 0.946, \text{ "high" } T_g\text{:}$$

$$T_g\ (°C) = 5.1 + 238W_B;\quad R(12) = 0.968$$

Obviously, these purely empirical linear correlations have no physical meaning since they rely on the overall copolymer composition (see further).

The occurrence of two transitions cannot be ascribed to strong compositional polydispersity effects, as already observed in some statistical copolymers,[24,25] since the chemical homogeneity of the samples is well documented.[1] It has to be considered an unambigous proof of the biphasic structure of the material, resulting from the aggregation of B units in B-rich microdomains of "high" T_g (hard phase, T_g^H) dispersed in a B-poor matrix of "low" T_g (soft phase, T_g^S). Assuming that the T_g^i in each ith phase obeys the Fox equation, as previously observed for the ethyl acrylate–zwitterionic system[3] (no more theoretically sound mixing law may be used because of the lack of data, especially ΔC_p values, for the B_n homopolymer; see further), a complete and quantitative description of the structure in terms of internal composition (weight fractions W_B^H and W_B^S) and relative importance of the hard and of the soft phases (weight fractions W^H and W^S and volume fractions Φ^H and Φ^S, respectively) may be easily derived from the following relations:

$$W_B^i = \frac{T_g(B_n)[T_g^i - T_g(A_n)]}{T_g^i[T_g(B_n) - T_g(A_n)]} \quad \text{with } W_A^i + W_B^i = 1$$

where i refers to the S (soft) or the H (hard) phase and $T_g(A_n)$ and $T_g(B_n)$ to the glass transition temperatures of the parent homopolymers.

$$W^H = \frac{W_B - W_B^S}{W_B^H - W_B^S} = \frac{W_A^S - W_A}{W_A^S - W_A^H} \quad \text{with } W^S + W^H = 1$$

The various W^H, W_B^S, and W_B^H values given in Table I were calculated taking the experimental DSC $T_g(A_n)$ value of −46 °C (literature data: −52 °C from dynamic mechanical spectroscopy[26]) and an estimated $T_g(B_n)$ value of about 255 °C.[27] Fortunately, the low accuracy of the T_g^H values only results in weak variations on the calculated compositional data: in the most unfavorable case such as for copolymer AB-7.1 ($T_g^H \pm 10$ °C), the fluctuations of W_B^H and W^H around their mean values are <10%.

The contribution of the B units to the heat capacity increment of the soft phase, ΔC_p^S, may be neglected in first approximation because their concentration remains very weak, <10% in most cases; moreover, the T_g^S variations cover a sufficiently narrow temperature range (about 20 °C) to consider the $\Delta C_p(A_n)$ values roughly constant,[28] identical to that measured at $T_g(A_n)$: $\Delta C_p(A_n) = 0.335\ J\ g^{-1}\ K^{-1}$ (literature value:[26] $0.322\ J\ g^{-1}\ K^{-1}$). Within these simplifying assumptions, the fraction of A units in the soft phase may be derived according to the ratio $R = (\Delta C_p^S/\Delta C_p(A_n))/W_A$ and compared with the value $W_A^S W^S/$

W_A. For B-poor copolymers ($W_B < 0.24$) the R ratio is only about 10% lower than the otherwise calculated value: this fairly good agreement (taking into account the accuracy of the ΔC_p measurements of about ±5%) may be considered an independent check on the reliability and of the self-consistency of the composition data derived from the T_g^i analysis, which implies the a priori choice of a model for the T_g^i dependence versus composition.

Three main structural features should be outlined for the biphasic copolymers.

(a) The progressive development of the hard phase is almost parallel with the overall increase of the zwitterion content in the copolymer. Its volume fraction reaches a maximum $\Phi^H = 0.50$ for copolymer AB-27.3, but it could probably become slightly predominant for samples within the range $0.28 < F_B < 0.48$ where the coexistence of two distinct transitions cannot be ascertained from our experimental results. However, for higher B contents, $F_B > 0.45$ ($W_B > 0.68$), no phase inversion (dispersion of soft microdomains in a hard matrix) can be detected: the copolymers appear monophasic again.

(b) The A and B units are obviously concentrated preferentially in the soft and hard phases, respectively, but with significant differences. The fraction of B rejected in the soft phase ($W_B{}^S W^S/W_B$) decreases from about 0.30 to 0.15 when W_B increases from 0.10 to 0.50. The molar fraction of B in the soft phase, $F_B{}^S$, remains always lower than 0.07, as expected from the lack of any solvation of the zwitterion by the alkyl acrylate units,[4] and the soft phase may thus appear fairly pure. On the other hand, the fraction of A rejected in the hard phase ($W_A{}^H W^H/W_A$) decreases from about 0.40 to 0.10 when W_A increases from 0.3 to 0.9. The mole fraction of A in the hard phase, $F_A{}^H$, is always higher than 0.45, becomes rapidly the major one for most of the samples ($W_B \leq 0.30$), and may reach values over 0.7 even for copolymers of relatively high B content ($W_B \leq 0.20$). The vicinal A segments chemically linked to the interacting zwitterionic B units are incorporated in the hard microdomains, which appear as a quite "mixed" phase.

(c) Addition of a stoichiometric amount of $LiClO_4$ to the copolymer ([$LiClO_4$]/[B] = 1) results in a completely amorphous blend (no trace of crystalline salt in the WAXS pattern) showing identical $T_g{}^S$ and a significantly increased $T_g{}^H$: see sample AB-7.1 + $LiClO_4$ in Table I. This feature suggests strongly preferential solvation of the ionic species in the hard phase, in good agreement with the already known complexation of various mineral salts by poly[(sulfopropyl)ammonium betaines][29] through specific ionic interactions.

Small- and Wide-Angle X-ray Scattering. The broad diffusion halo observed in WAXS patterns at about 1.1 nm for relatively B-poor copolymers is very similar to that observed for the A_n homopolymer, and it may be ascribed to interchain interactions between A blocks, as generally observed for alkyl acrylate polymers;[30] it vanishes for F_B values between 0.12 and 0.16, corresponding to an average n-butyl acrylate sequence length of about 9.

The SAXS patterns were recorded between room temperature and 180 °C for scattering vectors q in the range 0.2–3 nm^{-1} ($q = 4\pi \sin\theta/\lambda$, where λ is the X-ray wavelength and 2θ the scattering angle).

For copolymers of low and moderate zwitterion content, $0.04 \leq F_B \leq 0.49$, the SAXS patterns show a single well-defined scattering peak corresponding to a Bragg spacing d between 3 and 8 nm ($d = 2\pi/q$): see Figure 3. This peak is very similar to that previously observed in the ethyl acrylate–zwitterionic system[2] ($0.12 \leq F_B \leq 0.36$), although

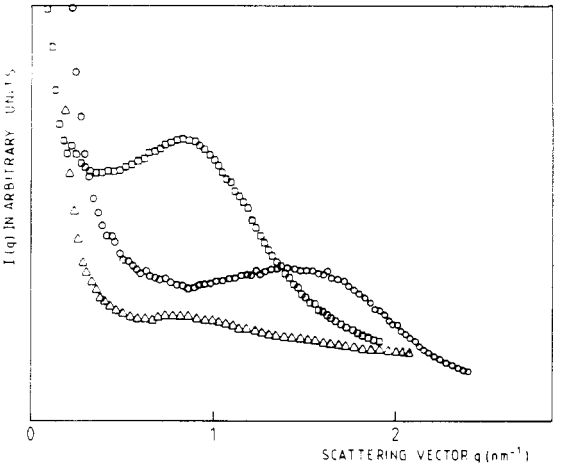

Figure 3. Representative SAXS profiles of some AB copolymers at room temperature: (△) AB-2.0; (□) AB-4.0; (○) AB-48.9.

it exists over a broader composition range, and it is highly reminiscent of the well-known "ionic" peak generally found in ionomers:[12-16] it merely reflects a periodic variation in electron density within the samples, and the lack of another maximum in the scattering profiles suggests a liquid-like order rather than any highly ordered structure. Moreover, the negligible variation of the product $q^3I(q)$ (linear collimation) observed at high q values is also consistent with a two-phase morphology and would suggest a rather sharp interface: however, this feature is uncertain since the experimental data are restricted to a narrow q range ($1.8 < q\ (nm^{-1}) < 3.0$). The influence of a number of parameters on the characteristic scattering peak has been probed.

(a) With respect to the zwitterion content, the SAXS peak appears slightly before the detection of the hard domains in DSC experiments and disappears simultaneously with the soft phase.

(b) Its sensitivity to the molecular weight distribution is probably very weak, since it is essentially identical for the polydisperse copolymer AB-12 ($M_w = 9.25 \times 10^4$, $M_w/M_n = 1.75$) and a narrower fraction ($M_w = 9.34 \times 10^4$, $M_w/M_n = 1.24$) of the same composition.

(c) Temperature effects depend on sample composition (Figure 4). For $F_B = 0.04$, the SAXS peak vanishes progressively between 100 and 130 °C, while for $F_B = 0.12$ a temperature increase from −40 to +180 °C results in a slight enhancement of the peak intensity, and a weak shift toward longer Bragg spacings ($d = 5.16$ and 5.68 nm at −40 and +180 °C, respectively): the peak remains clearly defined in the liquid state at about 120 °C above the $T_g{}^H$, and temperature effects are not completely reversible since the SAXS maximum remains slightly more intense when cooling the sample to 25 °C. The thermal history of the copolymers and their potential annealing at a given temperature may influence the SAXS patterns as already observed for some ionomers,[31] but their systematic study is beyond the scope of the present work.

(d) Addition of stoichiometric amounts of $LiClO_4$ ([$LiClO_4$]/[B] = 1) to copolymer AB-7.1 does not alter significantly the Bragg spacing, $d = 6.35 \pm 0.08$ nm, which is practically independent of temperature between 25 and 150 °C.

(e) Increasing the zwitterion content of the copolymer results in a simultaneous broadening of the peak and a decrease of the Bragg spacings from about 8 to 3 nm (see further discussion).

In spite of a number of theoretical and experimental approaches, the origin of the "ionic" SAXS peak in ionomers still remains a controversial topic.[13] However,

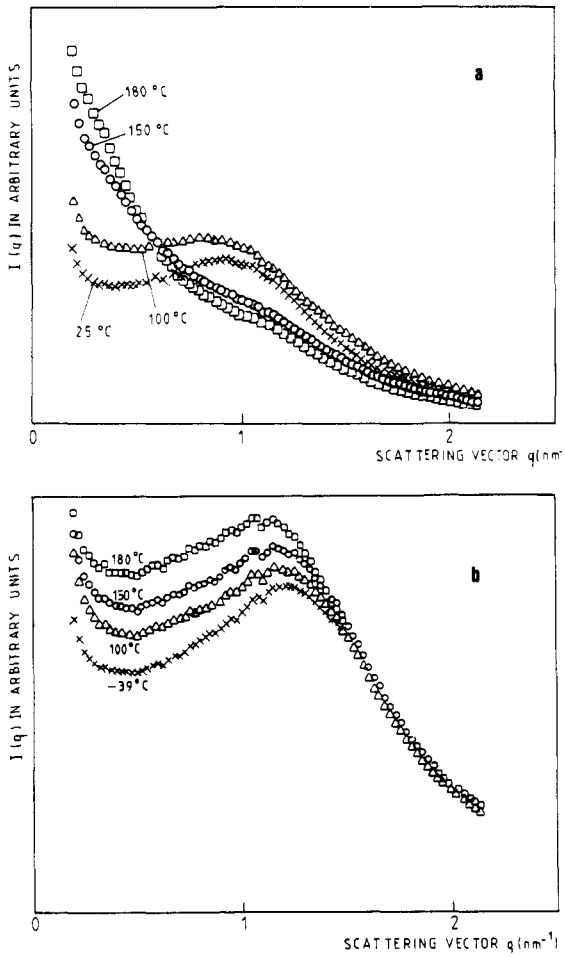

Figure 4. Temperature effects on the SAXS patterns of copolymers AB-4.0 (a) and AB-12.0 (b).

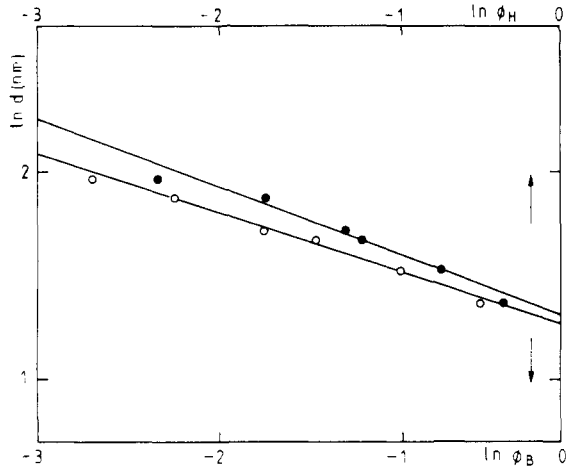

Figure 5. Variations of the SAXS average correlation distance d (nm) with the volume fraction of B units, Φ_B (○), or of the hard domains, Φ_H (●), in the copolymers.

according to most authors,[16] it may be ascribed to interparticle rather than intraparticle interferences, and the d spacings may be thus interpreted as the correlation distances between the centers of the scattering entities dispersed in the surrounding matrix. As shown in Figure 5, the d variations with composition obey a power law of the type $d \propto \Phi_B^{-0.27}$, as compared with $d \propto W_B^{-0.28}$ for the closely related zwitterionic–ethyl acrylate system[2] ($0.12 \leq F_B < 0.36$) and with $d \propto W_B^{-0.21}$ for sulfonated polystyrene ionomers[31] ($0.014 < F_{ion} \leq 0.055$). The oversimplified structural model which assumes quantitative and selective segregation of the B units in chemically pure microdomains of constant size randomly distributed within the A matrix leads to a power law[13] $d \propto \Phi_B^{-1/3}$. An alternative interpretation would be to consider the hard microdomains previously identified in DSC experiments as the scattering entities: the experimental data lead in this case to an analogous power law, $d \propto (\Phi^H)^{-0.31}$.

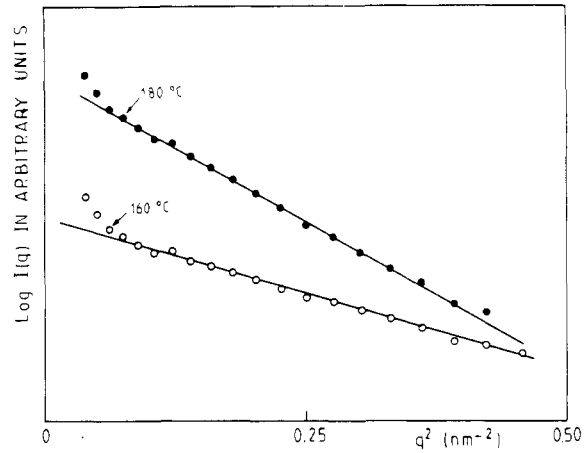

Figure 6. Guinier plot of the SAXS experimental data for copolymer AD-4.0 at 160 (○) and 180 °C (●).

It would be of great interest to derive the size of the scattering entities (radius of gyration R_g) from a Guinier analysis of the experimental data obtained at low values of the scattering vector q ($\ln I(q) = -R_g^2q^2/3$, where I is the scattered intensity): unfortunately, the overlap with the "ionic" peak is too important, and its contribution to the overall SAXS profile can never be safely neglected. However, in a first approach a Guinier analysis was performed on the data obtained at high temperature on the copolymer of the lowest B content ($F_B = 0.04$), where the peak disappears at 130 °C while a strong scattered intensity still persists: straightforward calculations (see Figure 6) lead to R_g values of about 1.38 and 1.95 nm at 160 and 180 °C, respectively, corresponding to a radius of 1.78 and 2.52 nm, assuming a spherical shape for the scattering entities which show no correlation because of their very low concentration. These primary values have to be considered quite cautiously, since significant deviations from the Guinier model may likely arise from nonuniformity in the size of the scattering particles. Moreover, there is no definite explanation for the observed rather strong temperature dependence.

To conclude with an oversimplified structural picture, a simple space-filling model leads to an average radius R for the spherical scattering microdomains distributed on a cubic lattice according to Φ_B or $\Phi^H = (4/3\pi R^3)/d^3$. Calculations show that the R variations are negligible over the whole composition range where the peak is observed ($0.04 < F_B < 0.49$): $R = 2.03 \pm 0.05$ or 2.24 ± 0.05 nm depending on the choice of Φ_B or Φ_H as the volume fraction of the scattering entities. Both R values are compatible with those derived from the Guinier analysis of the experimental data. The greater dimensions calculated for the hard phase merely reflect that the scattering microdomains involve significant amounts of A units in this case. The number of B units in these spherical hard microdomains would increase from about 50 to 100 for copolymers within the range $0.046 < F_B < 0.273$.

It is clear that the SAXS results alone cannot provide more reliable structural parameters. It may be emphasized that if the Bragg spacings are quite compatible with those generally observed in ionomers (studied in most cases for

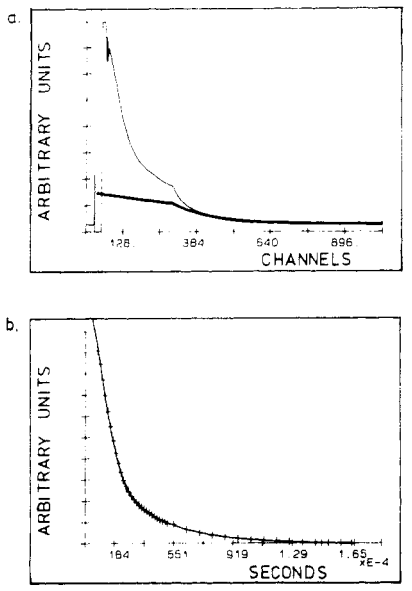

Figure 7. ^{1}H FID of copolymer AB-27.3 at 37 °C. Part a (thin line) shows the signal. The first 300 points are digitized at 5 MHz and the following one at 1 MHz. The signal is decomposed in three components: part b shows the initial part (170 μs) fitted with the sum of a Gaussian (49.5% of the signal, T_2 = 11.2 μs or M_2 = 11 G^2) and an exponential (34.8% of the signal, T_2 = 33 μs); the thick line in part a shows the slowest decaying component (exponential corresponding to 15.6% of the signal, T_2 = 123 μs).

molar ionic fractions lower than 0.15), the estimated R dimensions of the scattering microdomains are significantly higher.[16] The greater bulkiness of the (sulfopropyl)-ammonium betaine compared to the usual alkali metal ion pairs and the antiparallel alignment of the dipoles in the aggregates[17] may account for this difference. As a further comparison, the dipolar microdomains in lamellar polysiloxane dizwitterionomers[5] have been shown to have a radius of gyration independent of the zwitterion content, of about 2.2 ± 0.2 nm.

Solid-State NMR. Two complementary techniques were used for the study of the mobile and rigid nuclei in the copolymers: wide-line ^{1}H NMR analysis as a direct, quantitative but nonselective method and high-resolution MAS ^{13}C NMR as an indirect, qualitative but selective method. Measurements were restricted to three copolymers of low and intermediate zwitterionic contents (F_B < 0.27) representative of both monophasic and biphasic structures as indicated by DSC.

^{1}H dipolar line shape analysis was performed over a broad temperature range from −50 to +220 °C. Typical free induction decays (fid's) were decomposed into components of exponential or Gaussian shape as shown in Figure 7. While the homopolymer A_n shows a sharp step decrease of the unique fast component (see Figure 9) corresponding to a T_g (taken conventionally at the middle of the step) of about −38 °C, the copolymers' FIDs are characterized by three widely different time constants: the faster (≃10 μs) may be ascribed to a rigid phase (second moment of M_2 of several gauss^2) and the slower ones (>30 μs) to mobile phases (Figure 7). The variations of the weighted average time constants of the intermediate and long components with temperature show the characteristic behavior of a thermally activated process: see, e.g., the Arrhenius plot given in Figure 8 for copolymer AB-27.3. However, the average values of the activation energy derived from the slopes of such diagrams (E_a ≃ 17, 15, and 6 kJ mol^{-1} for copolymers AB-4, AB-12, and AB-27.3, respectively) have to be considered quite cautiously as regards their true physical meaning.[32]

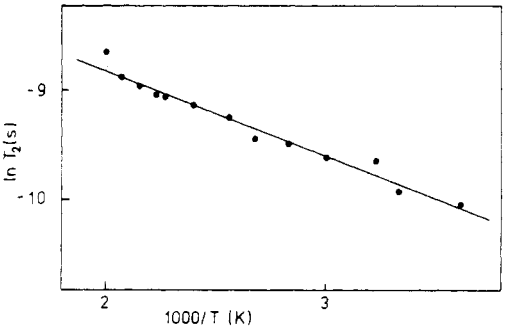

Figure 8. Temperature dependence of the weighted average time constants (T_2) of the exponential components plotted in an Arrhenius form for copolymer AB-27.3.

For a given copolymer at a given temperature, extrapolation of the data to the fid time origins yields directly the relative importance of the coexisting phases of distinct rigidity; this procedure allows us to derive a structural map giving the sample composition in terms of fractions (measured in H nuclei) of the rigid, intermediate, and mobile phases at any temperature (Figure 9). A number of interesting features may be outlined from the comparative analysis of these structural maps with the DSC results (Table II).

(a) The first fairly sharp decrease in the rigid fraction occurring at low temperature allows us to define a corresponding low T_g (conventionally taken at the middle of the transition) which may be directly correlated with the T_g^S previously observed in DSC. The shift toward higher temperature (20–40 °C) for NMR measurements reflects the difference of the two methods with respect to their frequency scale.

(b) The second decrease of the rigid fraction occurring at high temperature is not so well defined, especially because of the persistence of a residual, weak but well-ascertained fraction of rigid phase at the highest practicable temperatures (see further) as clearly shown, e.g., by the still fairly high value of the second moment M_2 of about 4.5 G^2 at 220 °C for copolymer AB-27.3 (Figure 10). The fraction of the rigid phase estimated within the temperature range between the two NMR transitions, Φ^R, would be directly correlated with the fraction of hard phase derived from DSC measurements Φ^H (after conversion using the H nuclei as the unit): the agreement experimentally observed for copolymers AB-12 and AB-27.3 (see Table II) is quite good and very gratifying. Since the NMR calculations are independent of any model, the self-consistency between the two sets of results may be considered a quantitative check on the DSC calculations. The intermediate phase identified in NMR belongs obviously to the soft phase identified in DSC.

(c) The residual rigid phase still stable at about 100 °C above their T_g^H (DSC) for copolymers AB-12 and AB-27.3 more especially may be tentatively correlated with the SAXS "ionic" peak remaining at these temperatures. Assuming that they are free from A units, an upper limit of the fraction of B units involved in these aggregates, τ, may be calculated and compared with the corresponding fraction of B units in the hard phase (DSC, $W_B{}^H W^H/W_B$) (Table II). Only a minor part of these zwitterions are still associated in rigid and very stable structures at such high temperatures.

The ^{13}C MR spectra allow us to obtain the composition of the phases of different mobilities.

(a) ^{13}C dipolar-averaged spectra at moderate spinning rates, as shown in Figure 11 for copolymer AB-4.0, are characteristic exclusively of the mobile phase. All the

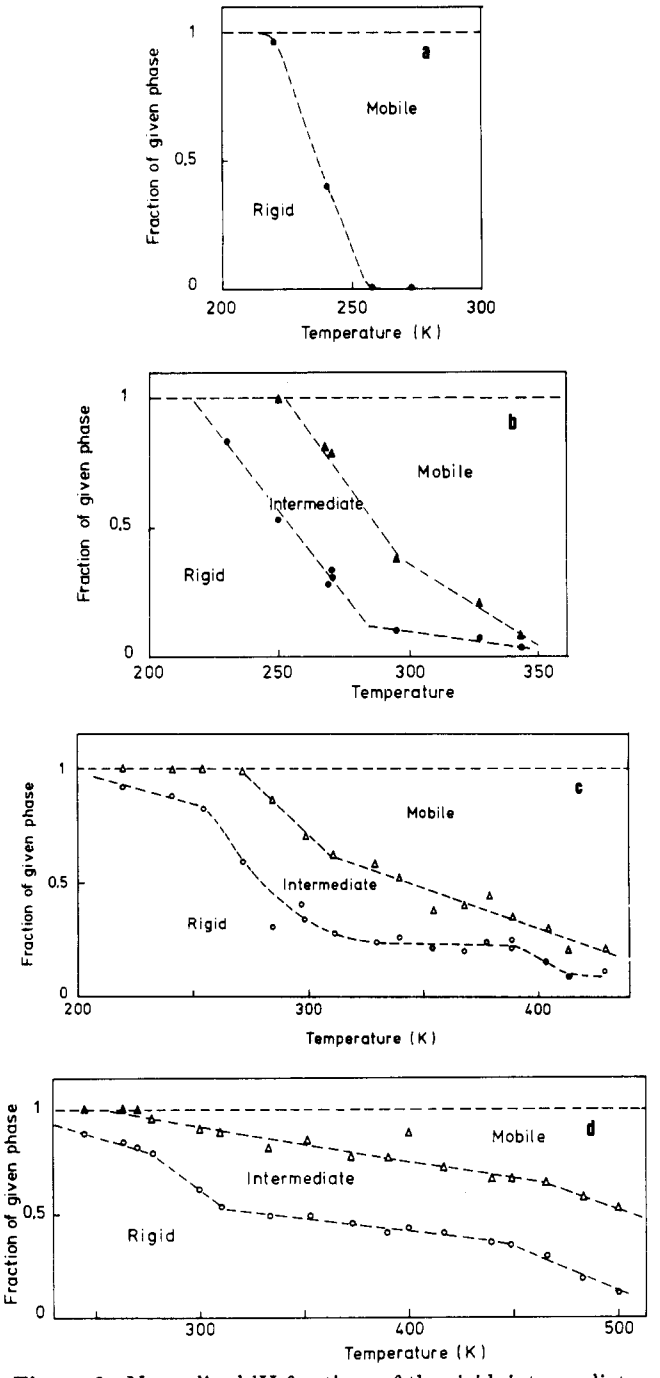

Figure 9. Normalized ^1H fractions of the rigid, intermediate, and mobile components at different temperatures for samples (a) A_n, (b) AB-4.0, (c) AB-12.0, and (d) AB-27.3.

spectra recorded under these experimental conditions are identical whatever the copolymer and correspond to that of poly(*n*-butyl acrylate) according to literature data[33] and by comparison with the ^{13}C NMR spectra obtained in $CDCl_3$ solution (solid-state spectra show a typical line broadening of about 5 ppm): the presence of B units cannot be detected in the limit of the method sensitivity, and this is in fairly good agreement with the very low amount of B units rejected into the soft phase as derived from DSC measurements (maximum value $F_B^S = 0.07$ for copolymer AB-27.3).

(b) ^{13}C–^1H cross-polarization spectra require strong dipolar interactions and thus allow the selective analysis of the rigid phase. At long contact times (2–5 ms) they show essentially the characteristic lines of the acrylate units A, and at shorter times (100–500 μs) additional resonances typical of the zwitterionic units B (identified by comparison with the high-resolution ^{13}C NMR spectrum of the homopolymer B_n in D_2O solution[34]) (Figure 11). The chemical heterogeneity of the rigid phase is thus well established.

(c) The technical capabilities of our ^{13}C NMR probe unfortunately do not allow polarization experiments above 100 °C, and the composition of the residual rigid phase stable at high temperature cannot be checked.

Structural Comparison of Butyl and Ethyl Acrylate Zwitterionomers. To summarize the preceding data, there is no doubt of a phase separation. The quantitative data of the relative importance and the composition of the coexisting phases and the persistence of a weak fraction of strongly interacting zwitterionic units in aggregates still stable at very high temperature in the liquid state may be considered as well documented on the basis of the self-consistency of the DSC, SAXS, and solid-state NMR experimental results. To the best of our knowledge, the occurrence of two well-separated T_g's in DSC measurements allowing the derivation of a fairly reliable structural model for the copolymers is unusual, if not unique, in the field of ionomers and zwitterionomers.

The much more pronounced phase separation observed in the butyl acrylate as compared to the ethyl acrylate betaine B′ copolymers studied previously[2-4] is worth emphasizing. It may be first tentatively ascribed to the different lengths of the spacer between the ammonium betaine and the chain backbone:

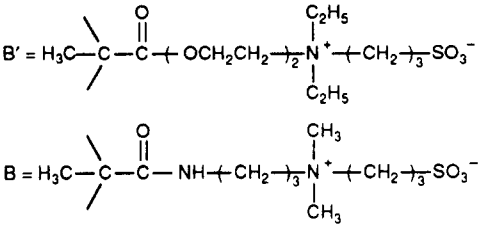

The influence of this factor should be significant according to recent results on styrene carboxylate ionomers of various structures.[35] However, it cannot be reliably predicted and it is probably not sufficiently important to account for the difference observed between the two copolymer systems. As a second potential factor, unit distribution is not identical in the two copolymer chains (see reactivity ratios[1,3]). Within the composition range $0.05 < F_{B,B'} < 0.45$, the average length of the zwitterionic blocks increases from about 1.1 to 2.0 for ethyl acrylate copolymers and from 1.1 to 2.3 for butyl acrylate copolymers. The slight increase of "blockiness" of the chain in the latter case may likely favor phase separation, but microstructure differences are probably not strong enough to account alone for the observed behavior. Variations of the polarity and thus of the solvation power of the matrices toward the zwitterionic units are expected to influence phase separation. Here again no definite conclusion may be drawn, since contradictory results are derived from dielectric and solvatochromic[29] measurements which lead to an average dipole moment $(\mu_0^2/N)^{0.5}$ and an "apparent local dipole moment" μ^* respectively of 1.0 D[36] and 2.7 D for poly(ethyl acrylate) and 1.8 D[19] and 2.1 D for poly(*n*-butyl acrylate). However, the μ^* values which arise from the polarity effects of the bulk polymer on the intramolecular charge-transfer transition of 4-ethylpyridinium dicyanomethylide chosen as a reporter probe[29,37] may probably be considered as better polarity parameters for the solvation of the zwitterionic units: the lower polarity

Table II
Comparison of DSC and Solid-State NMR Experimental Results

	DSC				NMR			
copolymer	T_g^S, °C	T_g^H, °C	Φ^H [a]	$(W_B^H W^H)/W_B$	T_g^S, °C	T_g^H, °C	Φ^R [a]	τ
AB-4	-40.1				-23	62 ± 5		<0.5[b]
AB-12	-32.7	63	0.28	0.72	-3	127	0.25	0.50
AB-27.3	-26	117	0.52	0.85	12	212 ● 5	0.45	0.36

[a] Φ^H and Φ^R are the fractions weighted in H atom of hard (DSC) and rigid (NMR) phases in the copolymer, respectively. [b] Very roughly estimated value because of the poor accuracy on the residual hard phase at 170 °C.

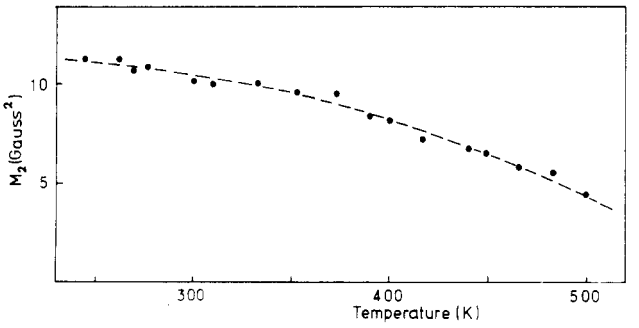

Figure 10. Variations of the second moment M_2 versus temperature for the copolymer AB-27.3.

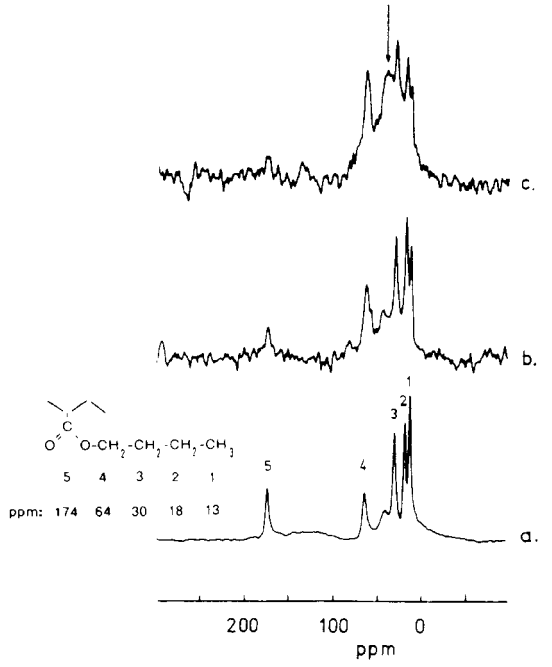

Figure 11. Solid-state ^{13}C-NMR high-resolution spectra of the copolymer AB-4.0 at 27 °C: (a) mobile phase; (b and c) rigid phase for a contact time of 2 ms and 500 μs, respectively. The arrow points to a peak characteristic of B units.

of the butyl acrylate matrix would thus enhance phase separation as expected. Obviously the greater ΔT_g difference between the two parent homopolymers in the butyl acrylate system ($\Delta T_g \simeq 300$ °C versus 150 °C in the ethyl acrylate copolymer) leads to a higher separation of the potential T_g^H and T_g^S. However, for a hypothetical ethyl acrylate copolymer analogous, e.g., to sample AB-12.8 ($T_g^S = -33$ °C, $T_g^H = +63$ °C) and showing soft and hard phases of identical molar composition, the T_g^S and T_g^H values (Fox equation) of respectively 1 and 70 °C would remain sufficiently separate to be clearly detected in DSC measurements: thus, the lack of two well-defined transitions cannot be ascribed to a too low sensitivity and accuracy of the technique. Finally, the high mobility of the butyl acrylate matrix ($T_g = -46$ °C) appears to be the decisive factor for the optimized phase separation experimentally observed: it allows the development of zwitterion-rich domains on a large enough scale to behave as an independent well-defined phase with its own glass transition. The strong analogy with cationic ionomers (4-vinylpyridinium methyl iodide) of butyl acrylate which are "clustered" copolymers[38] while those of ethyl acrylate only show "multiplet" associations[39] is especially striking.

Conclusion

As anticipated (see Introduction), the statistical zwitterionic butyl acrylate copolymers, readily obtained by radical copolymerization of industrial monomers,[1] provide very interesting polymeric materials reminiscent of the "clustered" ionomers.[12-16] Their morphology is in good agreement with the new multiplet-cluster model recently proposed by Eisenberg and al.:[40] when increasing the dipolar unit content, the microdomains of increased rigidity surrounding the multiplets progressively overlap into clusters of sufficient size to show their own high glass transition temperature. Although the general trends of the phase separation are well documented, a number of important questions still remain to be answered: geometry (shape, dimensions), polydispersity and distribution of the hard microdomains in the soft matrix, and organization of the dipolar units within the hard phase. These difficult problems have been already approached on low molecular weight model compounds[17] and on semitelechelic and telechelic zwitterionic polyisoprenes,[11] but a straightforward transposition to statistical copolymers is probably hazardous because of quite different steric constraints around the interacting dipolar structures. Forthcoming papers will tentatively address these topics through ^{13}C CP/DD/MAS NMR (study of the $T_{1\rho}(^1H)$ relaxations versus temperature for the rigid phase), SAXS analysis of the copolymers preferentially plasticized by apolar or dipolar solvents, and dynamic mechanical properties. Finally, sufficient experimental data have been collected to consider the "zwitterionomers" of the (sulfopropyl)ammonium betaine type as a versatile and promising alternative to the more classical ammonium cationic ionomers because of their greater thermal stability[41] and of their at least equal ability to yield microphase-separated materials of potential technological interest.

Acknowledgment. We gratefully acknowledge Rhône-Poulenc for a grant to one of us (M.E.) and for fruitful discussions with Drs. D. Charmot, J. C. Daniel, and R. Reeb.

References and Notes

(1) Ehrmann, M.; Galin, J. C. *Polymer*, in press.
(2) Mathis, A.; Zheng, Y. L.; Galin, J. C. *Makromol. Chem., Rapid Commun.* **1986**, *7*, 333.
(3) Zheng, Y. L.; Galin, M.; Galin, J. C. *Polymer* **1988**, *29*, 724.
(4) Bazuin, C. G.; Zheng, Y. L.; Muller, R.; Galin, J. C. *Polymer* **1989**, *30*, 654.
(5) Graiver, D.; Litt, M.; Baer, E. *J. Polym. Sci., Polym. Chem. Ed.* **1979**, *17*, 3573.

(6) Graiver, D.; Litt, M.; Baer, E. *J. Polym. Sci., Polym. Chem. Ed.* **1979**, *17*, 3607.
(7) Salamone, J. C.; Mahmud, N. A.; Mahmud, M. U.; Nagabhushanam, T.; Watterson, A. C. *Polymer* **1982**, *23*, 843.
(8) Clough, S. C.; Cortelek, D.; Nagabhushanam, T.; Salamone, J. C.; Watterson, A. C. *Polym. Eng. Sci.* **1984**, *24*, 385.
(9) Salamone, J. C.; Elayaperumal, P.; Clough, S. C.; Watterson, A. C.; Bibbo, M. A. *Polym. Prepr. (Am. Chem. Soc., Div. Polym. Chem.)* **1986**, *27*, 323.
(10) Neculescu, C.; Clough, S. C.; Elayaperumal, P.; Salamone, J. C.; Watterson, A. C. *J. Polym. Sci., Polym. Lett. Ed.* **1987**, *25*, 201.
(11) Fetters, L. J.; Graessley, W. W.; Hadjichristidis, N.; Kiss, A. D.; Pearson, D. S.; Younghouse, L. B. *Macromolecules* **1988**, *21*, 1644.
(12) Eisenberg, A.; King, M. *Ion Containing Polymers*; Academic Press: New York, 1977.
(13) MacKnight, W. J.; Earnest, T. R. *J. Polym. Sci., Macromol. Rev.* **1981**, *16*, 41.
(14) Bazuin, C. G.; Eisenberg, A. *Ind. Eng. Chem. Prod. Res. Dev.* **1981**, *20*, 271.
(15) Mauritz, K. A. *J. Macromol. Sci., Rev. Macromol. Chem. Phys.* **1988**, *C-28*, 65.
(16) Fitzgerald, J. J.; Weiss, R. A. *J. Macromol. Sci., Rev. Macromol. Chem. Phys.* **1988**, *C-28*, 99.
(17) Bredas, J. L.; Chance, R. R.; Silbey, R. *Macromolecules* **1988**, *21*, 1633.
(18) Chapoton, Y.; Galin, J. C.; Galin, M., unpublished results.
(19) Miklailov, G. P.; Burshtein, L. L. *Vysokomol. Soedin.* **1962**, *4*, 270.
(20) Guillon, D.; Mathis, A.; Skoulios, A. *J. Phys. (Les Ulis, Fr.)* **1975**, *36*, 695.
(21) Andersson, G. R. *Ark. Kemi* **1963**, *20*, 513.
(22) Meurer, B.; Spegt, P.; Weill, G. *J. Phys. E, Sci. Instrum.* **1983**, *16*, 403.
(23) Weiss, R. A.; Lundberg, R. D.; Turner, S. R. *J. Polym. Sci., Polym. Chem. Ed.* **1985**, *23*, 549.
(24) Ovchinnikov, E. Yu.; Gorelov, Yu. P. *Int. Polym. Sci. Technol.* **1989**, *16*, T/91.
(25) Guillot, J. *Makromol. Chem., Macromol. Symp.* **1990**, *35–36*, 269.
(26) Mathot, V. B. F. *Polymer* **1984**, *25*, 579.
(27) Because of thermal degradation, $T_g(B_n)$ was extrapolated from DSC measurements performed on the poly(zwitterion) plasticized by minute amounts of water: Galin, J. C.; Galin, M. *J. Polym. Sci., Polym. Phys. Ed.*, in press.
(28) Wunderlich, B.; Gaur, U. *Polymer Characterization: Spectroscopic, Chromatographic, and Physical Instrumental Methods*; Advances in Chemistry Series 203; Craver, C. D., Ed.; American Chemical Society: Washington, DC, 1983; p 195.
(29) Galin, M.; Marchal, E.; Mathis, A.; Meurer, B.; Monroy Soto, Y. M.; Galin, J. C. *Polymer* **1987**, *28*, 1937.
(30) Plate, N. A.; Shibaev, V. P. *J. Polym. Sci., Macromol. Rev.* **1974**, *8*, 117.
(31) Weiss, R. A.; Lefelar, J. A. *Polymer* **1986**, *27*, 3.
(32) Fedotov, V. D.; Schneider, H. Structure and Dynamics of Bulk Polymers by NMR Methods. *NMR: Basic Prin. Prog.* **1989**, *21*.
(33) Voelkel, R. *Angew. Chem., Int. Ed. Engl.* **1988**, *27*, 1468.
(34) Ehrmann, M.; Galin, J. C.; Meurer, B., results to be published.
(35) Moore, R. B.; Bittencourt, D.; Gauthier, M.; Williams, C. E.; Eisenberg, A. *Macromolecules* **1991**, *24*, 1376.
(36) Pohl, H. A.; Zabusky, H. H. *J. Phys. Chem.* **1962**, *66*, 1390.
(37) Lopez Velasquez, D.; Galin, J. C. *Macromolecules* **1986**, *19*, 1096.
(38) Duchesne, D.; Eisenberg, A. *Can. J. Chem.* **1990**, *68*, 926.
(39) Duchesne, D.; Eisenberg, A. *Polym. Prepr. (Am. Chem. Soc., Div. Polym. Chem.)* **1984**, *25* (2), 116.
(40) Eisenberg, A.; Hird, B.; Moore, B. *Macromolecules* **1990**, *23*, 4098.
(41) Gauthier, S.; Duchesne, D.; Eisenberg, A. *Macromolecules* **1987**, *20*, 753.

Registry No. AB (copolymer), 139131-56-9.